18th World IMACS / MODSIM Congress, Cairns, Australia 13-17 July 2009
http://mssanz.org.au/modsim09

Parametric behavior of the optimal control solution for collision avoidance in a close proximity encounter

Tarnopolskaya, T. [1] **and N. Fulton** [2]

[1] *CSIRO Mathematical & Information Sciences, North Ryde, New South Wales*
[2] *CSIRO Mathematical & Information Sciences, Canberra, Australian Capital Territory*
Email: tanya.tarnopolskaya@csiro.au

Abstract: This paper studies close proximity aircraft encounters that can occur in the missed-approach, in the circuit area, and for operations outside controlled airspace where air traffic management services may be unavailable and where aircraft may routinely fly in close proximity. The paper presents a synthesis of optimal control for cooperative collision avoidance strategies in a close proximity coplanar encounter and studies its behavior with change in system parameters. The aim of the paper is to derive a benchmark solution against which practical cases can be assessed.

The problem is formulated as a Mayer problem with free terminal point for a continuous control system. The control functions are the non-dimensional turn rates of the aircraft which are scaled so that they are bounded by ± 1, with positive values corresponding to the right turns and negative values corresponding to the left turns. The objective is to maximize the terminal miss distance on the trajectories with decreasing relative distance between the aircraft. The domain of the non-dimensional control system consists of two parts: (1) the non-dimensional state-vector $\boldsymbol{\rho}^T = (r, \phi, \theta)$ that specifies the instantaneous relative positions and relative direction of motion of two aircraft, and (2) the non-dimensional parameters of the problem γ and ω, which represent the ratios of the linear speeds and of the maximum turn rates respectively.

To date, analytic solutions were available only for the case of identical aircraft $\gamma = \omega = 1$ (the problem was first studied by Merz, and a rigorous analysis has been presented in the authors' recently published paper).

The focus of this paper is on a more general case $\omega \neq 1, \gamma = 1$ (the aircraft with unequal turn capabilities). The analysis is based on the Pontryagin Maximum Principle for a Mayer problem. The analytic solutions for the extremals are presented and the synthesis of optimal control is constructed based on the properties of the extremals. The analytic solutions make it possible to present the optimal control solution in a parametric form and study its behavior over a wide range of the parameter values. The analysis shows that the structure of the optimal control solution is significantly more complex in this more general case than in the case of identical aircraft. Thus, Merz' solution for identical aircraft represents a degenerate case of this more general solution.

The partitioning of the plane of initial conditions into the regions of initial conditions for different optimal strategies is determined and its change with the change in the non-dimensional parameter ω is established.

The closed form optimal control solutions and the analysis of their behavior with change in the non-dimensional parameter ω developed in this paper are useful for benchmarking and validating the performance of automated proximity management collision avoidance systems.

Keywords: *Optimal control, Pontryagin Maximum Principle, Mayer problem, close proximity, cooperative maneuvers, collision avoidance, analytic solutions*

1. INTRODUCTION

The growth in demand for air travel, and the introduction of aerial vehicle operations (without a human pilot) and personalised jets will result in increase in the frequency of aircraft proximity incidents. Some examples of operations where close proximity situations may occur include the missed approach, the circuit area, and operations outside controlled (managed) airspace where air traffic management (ATM) services may be unavailable and where aircraft routinely fly in closer proximity. Such situations require dependable proximity management at physical limits well below the more commonly understood ATM separation standards used in the present managed (controlled) airspace or those presently proposed for Free Flight airspace. As a result, there is a need to re-examine the physical and mathematical basis for existing proximity models and the present rules of the air.

While an advance in numerical optimization techniques makes it possible to study complex scenarios involving many participants (see Tarnopolskaya & Fulton, 2009a, for a comprehensive list of references), the analytic solutions for simplified scenarios are important as they have a potential to reveal the underlying structure of the solution and its behavior over a wide range of the parameter values.

This paper studies the cooperative coplanar close proximity encounter of two aircraft with equal linear speeds but unequal turn capabilities. The underlying assumption is that the linear speeds of the participants are constant (which is a reasonable assumption given a short time of the conflict).

The non-dimensional equations of motion in the moving polar coordinate system connected with the faster aircraft are (Merz, 1973a and 1973b; Tarnopolskaya and Fulton, 2009a)

$$\dot r = -\cos\phi + \cos(\theta-\phi), \quad \dot\phi = -\sigma_1 + [\sin\phi + \sin(\theta-\phi)]/r, \quad \dot\theta = -\sigma_1 + \omega\sigma_2, \tag{1}$$

where r, ϕ, θ specify the non-dimensional instantaneous relative distance between the aircraft and the instantaneous angles defining the relative direction of motion of two aircraft (see Figure 1); σ_1, σ_2 are the non-dimensional angular speeds of the aircraft scaled so that they are contained in the interval [-1, 1], with positive values corresponding to the right turns (from the point of view of the pilot), and negative values corresponding to the left turns; $\omega = |\omega_{2,\max}|/|\omega_{1,\max}| > 0$, where $\omega_{1,\max}, \omega_{2,\max}$ are the physical bounds of the angular speeds of the aircraft. The derivatives with respect to the non-dimensional time *t* are denoted with dots.

The system of ordinary differential equations (1) can be viewed as a control system with the state vector $\boldsymbol{\rho}^T = (r, \phi, \theta)$ and control function $\mathbf{u}^T = (\sigma_1, \sigma_2), \mathbf{u} : [0, T] \to U;\ U \subseteq IR^2$,

$U = [-1,1] \times [-1,1]$. The maximisation of terminal miss distance (the smallest distance between the participants during the maneuver) is adopted in this study as a performance criterion.

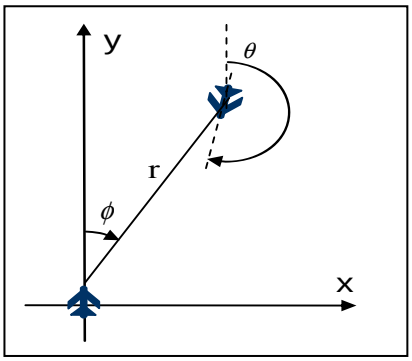

Figure 1: Schematics of the conflict in the moving reference frame

The important sub-class of the problem for ω =1 (identical aircraft) was first studied by Merz (Merz, 1973), and a rigorous analysis presented in Tarnopolskaya & Fulton, 2009a. This paper considers the case of aircraft with different turn capabilities (that is, $\omega > 0$). The analytic solutions developed by the authors are presented (a detailed analysis is given elsewhere (Tarnopolskaya & Fulton, 2009b)). They are used to study the structure and the behavior of the optimal control solution for a wide range of the parameter values ω.

1. OPTIMISATION PROBLEM

The non-dimensional maneuver time T (also known as the terminal time) is defined as the time of closest approach between the two aircraft. It is defined by the conditions

$$\dot r(T) = 0, \qquad \dot r(t) < 0, \qquad t \in [0, T]. \tag{2}$$

The control system is

$$\dot{\boldsymbol{\rho}} = f_p(\boldsymbol{\rho}, \mathbf{u}) = [-\cos\phi + \cos(\theta - \phi), \quad -\sigma_1 + [\sin\phi + \sin(\theta - \phi)]/r, \quad -\sigma_1 + \omega\sigma_2]^T, \ \boldsymbol{\rho}\big|_{t=0} = \boldsymbol{\rho}_0, \tag{3}$$

and the objective is to maximize the terminal miss distance $\psi(\boldsymbol{\rho}, \mathbf{u}) = r\big|_{t=T} \equiv r_T$ over all admissible controls. Therefore, the performance index is a function of the terminal time only. As the terminal time T is unknown, the problem can be considered as a Mayer problem with free terminal point.

We also define, for the sake of definiteness, the domains for the state variables within the range

$$0 \le \theta < 2\pi, \qquad -\pi \le \phi < \pi. \tag{4}$$

It is easy to see that the first of Eqs.(2) together with Eqs.(3) yield two possible terminal conditions:

1. $\theta_T = 0$; (5)

2. $\phi_T = \theta_T/2 - \pi, \quad \phi_T = \theta_T/2.$ (6)

2. NECESSARY CONDITIONS FOR OPTIMALITY

The Hamiltonian function in the polar coordinate system is given by:

$$H(\boldsymbol{\lambda}(t), \boldsymbol{\rho}(t), \mathbf{u}(t)) = \boldsymbol{\lambda}^T \bullet f_p(\boldsymbol{\rho}, \mathbf{u}) = \lambda_r(t)\dot{r}(t, \mathbf{u}) + \lambda_\phi(t)\dot{\phi}(t, \mathbf{u}) + \lambda_\theta(t)\dot{\theta}(t, \mathbf{u})$$

$$= \lambda_r[-\cos\phi + \cos(\theta - \phi)] + \lambda_\phi\{-\sigma_1 + [\sin\phi + \sin(\theta - \phi)]/r\} + \lambda_\theta(-\sigma_1 + \omega\sigma_2), \tag{7}$$

where the adjoint variables $\boldsymbol{\lambda}^T(t) \equiv (\lambda_r(t), \lambda_\phi(t), \lambda_\theta(t))$ satisfy the equations

$$\dot{\boldsymbol{\lambda}} = -\nabla H = \begin{bmatrix} \lambda_\phi[\sin\phi + \sin(\theta - \phi)]/r^2 \\ -\lambda_r(\sin\phi + \sin(\theta - \phi)) - \lambda_\phi[\cos\phi - \cos(\theta - \phi)]/r \\ \lambda_r \sin(\theta - \phi) + \lambda_\phi \cos(\theta - \phi)/r \end{bmatrix} \tag{8}$$

with boundary conditions $\boldsymbol{\lambda}(T) = \nabla\psi(\boldsymbol{\rho}(T), \mathbf{u}) = [1, 0, 0]^T$.

Using the Pontryagin Maximum Principle (Pontryagin et al., 1965), it can be shown (Tarnopolskaya & Fulton, 2009b) that the terminal conditions (5) and (6) yield two types of possible optimal strategies: 1) terminal condition (5) corresponds to $\sigma_1 = -\sigma_2 = \pm 1$ (the aircraft are turning with maximum angular speed in opposite directions). We will call these strategies right-left (RL) and left-right (LR) strategies; 2) terminal condition (6) results in $\sigma_1 = \sigma_2 = \pm 1$ (both aircraft are turning with the maximum angular speed in the same directional sense). Such strategies will be called right-right (RR) and left-left (LL) strategies.

Using the transformation of variables $r = \sqrt{x^2 + y^2}$, $r\sin\phi = x$, $r\cos\phi = y$, Eq. (1) can be re-written in the Cartesian coordinates and presented in terms of backward (retrograde) derivatives as

$$\overset{\circ}{x} = \sigma_1 y - \sin\theta, \qquad \overset{\circ}{y} = 1 - \sigma_1 x - \cos\theta, \qquad \overset{\circ}{\theta} = \sigma_1 - \omega\sigma_2. \tag{9}$$

Solving Eqs.(9) subject to the boundary conditions $x\big|_{\tau=0} = x_T$, $y\big|_{\tau=0} = y_T$, and one of the two terminal conditions (5), (6) yields the following cases:

Case I. $\theta_T = 0$, $\sigma_1 = -\sigma_2 = \pm 1$. This case corresponds to the RL and LR strategies.

The solution of Eqs. (9) is given by

$$\begin{aligned} \theta &= \begin{cases} \sigma_1(1+\omega)\tau & \text{for} \quad \sigma_1 = 1, \\ 2\pi + \sigma_1(1+\omega)\tau & \text{for} \quad \sigma_1 = -1, \end{cases} \\ x &= r_T \sin(\phi_T + \sigma_1\tau) + \sigma_1[1 + \cos[(1+\omega)\tau]/\omega - (1+\omega)\cos\tau/\omega], \\ y &= r_T \cos(\phi_T + \sigma_1\tau) + (1+\omega)\sin\tau/\omega - \sin[(1+\omega)\tau]/\omega, \end{aligned} \tag{10}$$

where subscript "T" refers to the terminal instant, τ is the backward time, $\tau = T - t$. For $\tau = T$, Eqs. (10) describe the loci of the initial conditions $(x_0 \equiv x|_{t=0}, y_0 \equiv y|_{t=0})$ and take the form

$$\text{For } \sigma_1 = 1: \quad \begin{aligned} &\{x_0 - 1 - \cos\theta_0 / \omega + (1+\omega)\cos[\theta_0/(1+\omega)]/\omega\}^2 \\ &+ \{y_0 - (1+\omega)\sin[\theta_0/(1+\omega)]/\omega + \sin\theta_0/\omega\}^2 = r_T^2 \end{aligned} \tag{11}$$

$$\text{For } \sigma_1 = -1: \quad \begin{aligned} &\{x_0 + 1 + \cos\theta_0 / \omega - (1+\omega)\cos[(\theta_0 - 2\pi)/(1+\omega)]/\omega\}^2 \\ &+ \{y_0 + (1+\omega)\sin[(\theta_0 - 2\pi)/(1+\omega)]/\omega - \sin\theta_0/\omega\}^2 = r_T^2 \end{aligned} \tag{12}$$

Case II. $\theta_T = 2\phi_T + 2\pi$ or $\theta_T = 2\phi_T$; $\sigma_1 = \sigma_2 = \pm 1$. This case corresponds to the RR and LL strategies.

The solution of Eqs. (9) takes the form

$$\begin{aligned} &\theta = \sigma_1(1-\omega)\tau + \theta_T, \quad y = r_T\cos(\phi_T + \sigma_1\tau) + \sin\tau - \sigma_1\{\sin(\theta_T + \sigma_1\tau) - \sin[\theta_T + \sigma_1(1-\omega)\tau]\}/\omega, \\ &x = r_T\sin(\phi_T + \sigma_1\tau) + \sigma_1\cos(\theta_T + \sigma_1\tau)/\omega + \sigma_1(1-\cos\tau) - \sigma_1\cos[\theta_T + \sigma_1(1-\omega)\tau]/\omega. \end{aligned} \tag{13}$$

For $\tau = T$ we have $\theta_0 = \sigma_1(1-\omega)T + \theta_T$, and the two branches of the initial conditions for the state variables (x, y) are given by:

$$\text{For } \phi_T = \theta_T/2: \begin{cases} [x_0 - \sigma_1(1-\cos\theta_0/\omega)]^2 + (y_0 - \sigma_1\sin\theta_0/\omega)^2 \\ = r_T^2 + 2 - 2\cos[\theta_0 - \sigma_1(1-\omega)T]/\omega - 2r_T\sigma_1(1+1/\omega)\sin[(\theta_0 - \sigma_1(1-\omega)T)/2], \end{cases} \tag{14}$$

$$\text{For } \phi_T = \theta_T/2 - \pi: \begin{cases} [x_0 - \sigma_1(1-\cos\theta_0/\omega)]^2 + (y_0 - \sigma_1\sin\theta_0/\omega)^2 \\ = r_T^2 + 2 - 2\cos[\theta_0 - \sigma_1(1-\omega)T]/\omega + 2r_T\sigma_1(1+1/\omega)\sin[(\theta_0 - \sigma_1(1-\omega)T)/2]. \end{cases} \tag{15}$$

3. SYNTHESIS OF OPTIMAL CONTROL

In order to select the optimal trajectories from the set of extremals, one should: (a) select the trajectories such that the distance between the aircraft decreases on $t \in [0, T]$; (b) amongst such trajectories, select those that maximize the performance criterion (the terminal miss distance). Firstly, consider the trajectories along which the distance between the aircraft decreases, that is

$$\dot{r} = 2\sin(\theta/2)\sin(\phi - \theta/2) < 0; \; t \in [0, T). \tag{16}$$

Inequality (16) yields, for the state variable θ within the range defined by Eq. (4): $\theta/2 - \pi < \phi < \theta/2, \quad t \in [0, T]$. For $t = 0$, the latter inequality reduces to

$$\theta_0/2 - \pi < \phi_0 < \theta_0/2. \tag{17}$$

It follows from Eq. (17) that the straight line $\tan\phi = \tan(\theta_0/2)$ divides the plane of the initial condition into the two sub-regions of the initial conditions for the trajectories with positive and negative instantaneous time derivative of the distance between the aircraft at the beginning of the maneuver.

Firstly, we present, without proof, several results that follow from the analysis of the properties of the extremals (for proofs, see Tarnopolskaya & Fulton, 2009b):

Proposition 1 *For $0 < \theta_0 < \pi$, possible optimal strategies include right-right(RR), left-left (LL) and right-left (RL) strategies. For $\pi < \theta_0 < 2\pi$, possible optimal strategies include right-right(RR), left-left (LL) and left-right (LR) strategies.*

Proposition 2 *Of all the loci of the initial conditions for RR and LL strategies described by Eqs. (14) and (15), only those described by Eq. (14) with $\sigma_1 = -1$ and Eq. (15) with $\sigma_1 = 1$, correspond to the trajectories with decreasing relative distance between the aircraft (that is, when condition (16) is satisfied). The direction of motion of the corresponding trajectories is clockwise towards $\phi_T = \theta_T/2$ for strategy associated with loci Eq. (14) $\sigma_1 = -1$ and is anticlockwise towards $\phi_T = \theta_T/2 - \pi$ for strategy associated with loci Eq. (15) with $\sigma_1 = 1$.*

Using the above results, we can now construct, for a given θ_0, the loci of initial conditions for x, y with associated strategies that deliver a given terminal miss-distance r_T and ensure a decreasing relative distance between the aircraft during the maneuver. We denote the loci by $R(r_T, \theta_0) \equiv \{x_0, y_0, \mathbf{u} : r\big|_{t=T} = r_T, \theta\big|_{t=0} = \theta_0\}$. We also define the internal envelope $\Re(r_T, \theta_0)$ of the loci with associated strategies $R(r_T, \theta_0)$ as: $\Re(r_T, \theta_0) \equiv \{(x_0^*, y_0^*, \mathbf{u}) : (x_0^*, y_0^*, \mathbf{u}) \in R(r_T, \theta_0);$ for any value ϕ, $r_\phi(x_0^*, y_0^*) = \min_{(x_0, y_0) \in R(r_T, \theta_0)} r_\phi(x_0, y_0)\}$. Consider the loci of initial conditions for the trajectories with decreasing relative distance defined above. Denote the point of intersection of the RR loci (15) and the LL loci (14) in polar coordinates by $\mathbf{r}^{(0)}(r_T, \theta_0) = (r^{(0)}(r_T, \theta_0), \phi^{(0)}(r_T, \theta_0))$. Also denote the point of intersection of the RR loci (15) and RL (LR) loci (Eq. (11) or (12)) by $\mathbf{r}^{(1)}(r_T, \theta_0) = (r^{(1)}(r_T, \theta_0), \phi^{(1)}(r_T, \theta_0))$. The point of intersection of the LL loci (14) and the RL (LR) loci (Eq. (11) or (12)) is denoted by $\mathbf{r}^{(2)}(r_T, \theta_0) = (r^{(2)}(r_T, \theta_0), \phi^{(2)}(r_T, \theta_0))$. We define the internal envelope $\Re(r_T, \theta_0)$ as follows:

$$\Re(r_T, \theta_0) = \begin{cases} \text{if} \quad r^{(0)} \le r^{(1)}, \ \text{arc of RR loci Eq.(15) for} \quad \theta_0/2 - \pi < \phi < \phi^{(0)}, \\ \qquad\qquad\qquad\quad \text{arc of LL loci Eq.(14) for} \quad \phi^{(0)} < \phi < \theta_0/2, \\ \\ \text{if} \quad r^{(0)} > r^{(1)}, \ \text{arc of RR loci Eq.(15) for} \quad \theta_0/2 - \pi < \phi < \phi^{(1)}, \\ \qquad\qquad\qquad\quad \text{arc of RL loci Eq.(11) for} \quad \phi^{(1)} < \phi < \phi^{(2)}, 0 < \theta_0 < \pi, \\ \qquad\qquad\qquad\quad \text{arc of LR loci Eq.(12) for} \quad \phi^{(1)} < \phi < \phi^{(2)}, \pi < \theta_0 < 2\pi, \\ \qquad\qquad\qquad\quad \text{arc of LL loci Eq.(14) for} \quad \phi^{(2)} < \phi < \theta_0/2. \end{cases} \tag{18}$$

The following results can be proved (Tarnopolskaya & Fulton, 2009b).

Lemma 1: *For each point (x_0, y_0) on the loci of initial conditions with associated strategies $R(r_T, \theta_0)$ that lies outside the internal envelope $\Re(r_T, \theta_0)$, there exists a strategy that delivers a terminal miss distance larger than r_T.*

Corollary: *The strategies associated with the initial conditions described by the internal envelope $\Re(r_T, \theta_0)$ are the optimal strategies for given initial conditions x_0, y_0, θ_0.*

For a given r_T and θ_0, the point on the plane of the initial conditions (x, y) that serves as the initial condition for two different optimal strategies that result in the same terminal miss distance is called a dispersal point. A loci of the dispersal points for a given θ_0 is called a dispersal curve. The dispersal curves partition the plane of the initial conditions into the sub-regions of the initial conditions for different optimal strategies. For a given θ_0, a triple point is a point on the plane of the initial conditions that corresponds to three different optimal strategies that result in the same terminal miss distance. Thus, the curve $\mathbf{r}^{(0)}(r_T, \theta_0)$ represents the RR-LL dispersal curve, while $\mathbf{r}^{(1)}(r_T, \theta_0)$ and $\mathbf{r}^{(2)}(r_T, \theta_0)$ are RR-RL and LL-RL dispersal curves respectively. The triple point is the point of simultaneous intersection of all three dispersal curves.

4. PARAMETRIC BEHAVIOR OF THE OPTIMAL CONTROL SOLUTION

We can now study the behavior of the solution with change in the non-dimensional parameter ω. Firstly, consider the behavior of the loci of the initial conditions for RR and LL strategies with change in ω. Main results can be summarized as follows:

Proposition 3 *For RR and LL strategies, the loci of the initial conditions for x, y, for a given θ_0 and r_T and varying time of encounter T, represent spirals. For $\omega = 1$ (Merz' solution for identical aircraft, Refs. 1-3), the spirals turn into circles with centers lying on the line passing through the origin and forming the angle $\theta_0/2$ with the vertical axis (counting clockwise from positive direction of y-axis). For $\omega > 1$, the spirals are bounded and contained between two concentric circles. As $\omega \to \infty$, the coordinates of the centers of spirals approach the point $(\sigma_1, 0)$, while the radii of the concentric circles bounding the spirals approach the values $R_{small} = r_T^2 + 2 - 2r_T$; $R_{large} = r_T^2 + 2 + 2r_T$. For $\omega < 1$, both the centers and the radii of the RR and LL spirals are unbounded and expanding as $\omega \to 0$.*

The behavior of the loci of the initial conditions is illustrated in Figure 2.

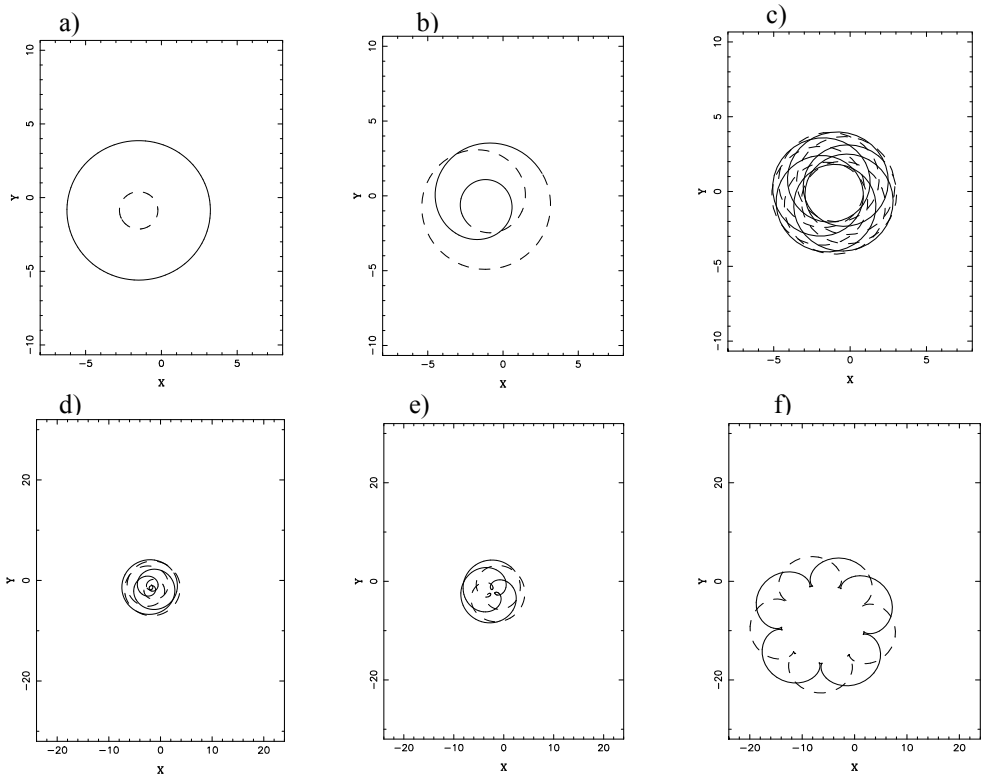

Figure 2: Transformation of the loci of initial conditions for LL strategies with change in ω, $\theta_0=2\pi/3$, $r_T=3$; Spirals corresponding to branches $\phi_T = \theta_T / 2$ and $\phi_T = \theta_T / 2 - \pi$ are shown with solid and dashed curves respectively; a) ω=1; b) ω=2; c) ω=10; d) ω=0.6; e) ω=0.4; f) ω=0.1 .

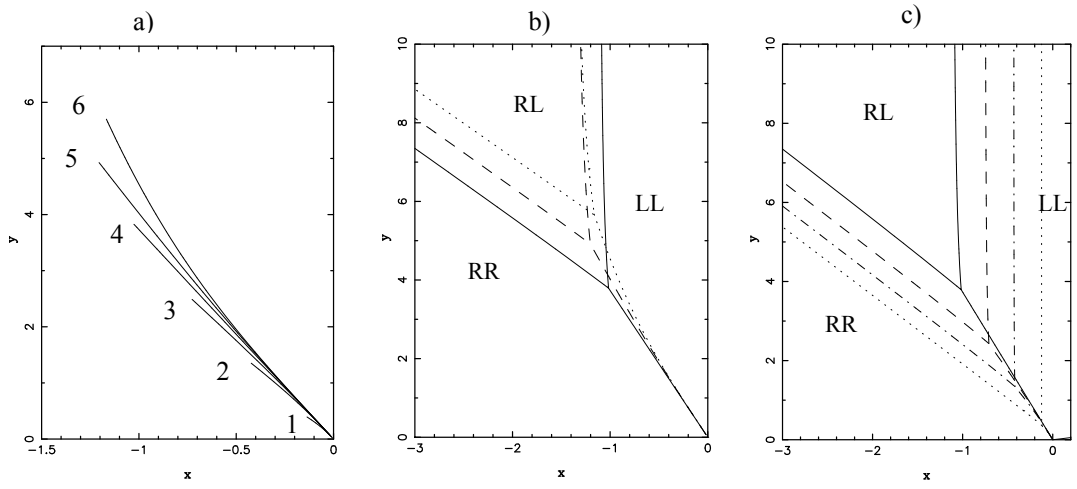

Figure 3: Dispersal curves for $\theta_0 = 5\pi/6$; a) RR-LL dispersal curves shown up to the triple point only; 1: ω = 15; 2: ω = 4; 3: ω = 2; 4: ω = 1; 5: ω = 0.5; 6: ω = 0.1; b) Dispersal curves and partition of the plane of initial positions into the regions of different optimal strategies for different values of parameter ω; _____ ω = 1; _ _ _ _ ω = 0.5; ……. ω = 0.1; c) Dispersal curves and partition of the plane of initial positions into the regions of different optimal strategies for different values of parameter ω; _____ ω = 1; _ _ _ _ ω = 2; _ . _ . _ . _ ω = 4; …… ω = 15.

We now consider the behavior of the dispersal curves and the triple point with change in ω. Figure 3a shows the RR-LL dispersal curves for values of r_T between zero and the triple point, and different values of ω. One can see that, with increase in ω, the radial position of the triple point decreases while the dispersal curves rotate anticlockwise. Figures 3b and3c show the partitioning of the plane of the initial conditions for x, y into the regions of different optimal strategies for $\theta_0 = 2\pi/3$ and different values of parameter ω. One can see that in all cases the plane of the initial conditions is partitioned into three sub-regions of different optimal strategies. Rather interestingly, while RR-LL dispersal curves rotate clockwise with decrease in ω, the RR-RL and LL-RL dispersal curves remain nearly parallel to themselves during the transformation. Also, RL-LL dispersal curves remain nearly parallel to y-axis, thus suggesting that a simple practical approximation for these dispersal curves is possible.

DISCUSSION AND CONCLUSIONS

The paper studies the parametric behavior of the optimal control solution for collision avoidance of aircraft with unequal turn capabilities in a close proximity encounter, based on the analytic solutions developed by the authors. The non-dimensional parameter of the problem is the ratio of the maximum turn rates of the aircraft ω. The analysis revealed that there are many common features of the optimal control solution for different values of ω. They are:

- the optimal strategies consist of combinations of the maximum and minimum values of the control functions and include right-right (RR), left-left (LL), right-left (RL) and left-right (LR) strategies;
- the partition of the plane of the initial conditions into sub-regions of the initial conditions for different optimal strategies has common structure. Thus, there are 3 sub-regions of different optimal strategies for a given θ_0. For $0 < \theta_0 < \pi$, they are right-right (RR), left-left (LL) and right-left (RL) strategies, while for $\pi < \theta_0 < 2\pi$ they are right-right (RR), left-left (LL) and left-right (LR) strategies;
- A presence of the triple point (a point where all three optimal strategies result in the same miss-distance) is a general feature of the solution for all values of the parameter.

Despite the common features of the optimal control solution, the structure of the optimal control solution in general case is significantly more complex than in the previously studied case of identical aircraft $\omega = 1, \gamma = 1$ (Merz, 1973; Tarnopolskaya & Fulton, 2009a). Thus, the loci of the initial conditions and the trajectories for the right-right (RR) and left-left (LL) strategies, which are spirals in a general case, degenerate into circles for $\omega = 1$. Also, while the regions of initial conditions for all optimal strategies change with time along the optimal path for the general case $\omega \neq 1$, the loci of initial conditions for the optimal RR and LL strategies remain stationary for $\omega = 1$. Thus, the well-known Merz' solution for identical aircraft represents a degenerate case of a more general solution. The geometry of the partitioning of the plane of the initial conditions into regions of different optimal strategy changes with change in ω. The non-dimensional radial coordinate of the triple point decreases with increasing ω. However, the dispersal curves remain nearly parallel to themselves with change in ω.

This papers derives a benchmark (ideal solution) against which practical solutions can be assessed. The results of this paper are useful for improving the understanding and control of the aircraft maneuvering in close proximity. The solutions developed are also useful for maritime applications and robotics.

REFERENCES

Bryson, A.E., Dynamic Optimization, Addison Wesley, California, 1999.

Merz, A.W. (1973a), Optimal Aircraft Collision Avoidance, Proc. Joint Automatic Control Conf., Paper 15-3, pp. 449-453.

Merz, A.W. (1973b), Optimal Evasive Manoeuvres in Maritime Collision Avoidance, *Navigation*, 20 (2), 144-152.

Pontryagin, L.S., Boltyanski, W.G., Gamkrelidze, R.V., and Mishchenko, E.F., The Mathematical Theory of Optimal Processes, John Wiley & Sons, New York, 1965.

Tarnopolskaya, T., and Fulton, N. (2009a), Optimal Cooperative Collision Avoidance Strategy for Coplanar Encounter: Merz's Solution Revisited, *Journal of Optimization Theory and Applications*, 140(2), 355-375.

Tarnopolskaya, T., and Fulton, N. (2009b), Synthesis of optimal control for collision avoidance of aircraft (ships) with unequal turn capabilities, *Journal of Optimization Theory and Applications*, accepted.